Applied Materials Today 4 (2016) 71–77

Contents lists available at ScienceDirect

Applied Materials Today

journal homepage: www.elsevier.com/locate/apmt

Short Communication

Fluorescent carbon nanodots for targeted *in vitro* cancer cell imaging

Sandhya Aiyer[a,1], Rajendra Prasad[b,1], Manoj Kumar[c], K. Nirvikar[c], Bhanprakash Jain[a], Omkar S. Kushwaha[d,*]

[a] *Polymer Science and Engineering Division, CSIR – National Chemical Laboratory, Pune 411008, India*
[b] *Catalysis Division, CSIR – National Chemical Laboratory, Pune 411008, India*
[c] *Metallurgical Engineering & Materials Science Department, IIT Bombay, Mumbai 400076, India*
[d] *Chemical Engineering & Process Development Division, CSIR – National Chemical Laboratory, Pune 411008, India*

ARTICLE INFO

Article history:
Received 23 May 2016
Received in revised form 8 June 2016
Accepted 13 July 2016

Keywords:
Green fluorescence
Carbon quantum/nano dots
Cancer cell bio-imaging
Targeting ability
Photoluminescence stability
Cell cytoplasm and nucleus targeting

ABSTRACT

Carbon quantum dots (CQDs or C-dots, ≤10 nm in size) are tiny carbon nanoparticles being envisaged in biosensing, bio-imaging and biomolecular/drug delivery. In the present investigation, green fluorescent carbon quantum/nano dots (GCQDs, ~3 nm in size) were synthesized through facile chemical slicing method. Further, folic acid (FA) functionalized GCQDs (GCQDs-FA) were obtained to enhance their targeting ability. FA is known to positively influence the binding potential and penetration into the cancer cells because of high abundance of folate receptors (FR) on various cancer cell membranes. We report high biocompatibility, photoluminescence stability and excellent *in vitro* cancer cell cytoplasm and nucleus targeting performance of GCQDs-FA on MCF-7 breast cancer cells.

© 2016 Elsevier Ltd. All rights reserved.

1. Introduction

Cancer is one of the deadliest human diseases [1] with over 10 million new cases reported every year [2]. The treatment of cancer is complex and requires targeted therapeutics along with a variety of nanoplatforms making it a thrust area of research [3,4]. Progress in biomedical fields [5,6] has taken early stage cancer diagnostics research to new dimensions [6–10] with great demand for high resolution optical imaging using organic dyes and inorganic nanoparticles (metal quantum dots) [11–15]. However, the use of various organic dyes and metal quantum dots as fluorescent probes for optical bioimaging [16–18] has been hampered due to poor photostability, low water solubility, high toxicity and low biocompatibility [19,20]. Recently, fluorescent carbon nanomaterials particularly quantum/nano dots has been materialized as the most attractive probes in nanomedicine [21–23] due to prolonged photostability, good water solubility, high biocompatibility and low toxicity [23–26]. In literature, number of publications with luminescence behavior of carbon quantum dots being obtained from various carbon sources by top-down and bottom-up approaches has been reported [27–38]. However, expensive precursors, long reaction time (2–3 days), sophisticated synthetic routes and harsh experimental conditions are barrier in the large scale synthesis of CQDs [37–44]. Additionally, large scale synthesis of photoluminescent carbon quantum dots within confined size limits (≤10 nm) with long-term photostability is still a challenge [45,46]. In the present investigation, we report an ambient large scale synthesis of green fluorescent carbon quantum/nano dots (GCQDs) and their potential application in early cancer diagnostics (Scheme 1). To obtain GCQDs, carbon fibers were subjected to chemical slicing. Here, we firstly report one pot large scale synthesis of GCQDs (>50% conversion efficiency) at ambient conditions. Folic acid (FA) was used as a targeting ligand to target the MCF-7 breast cancer cells through receptor mediated endocytosis. FA is a commonly used targeting ligand because of low molecular weight, good water solubility, high biocompatibility and over expression of folate receptors (FRs) on lung, breast, ovarian and renal cancer cells [47,48]. GCQDs-FA exhibited good biocompatibility and targeting ability leading to its high deep intracellular uptake and potential applications in cancer cell imaging. Additionally, we also report dual targeting ability of folic acid functionalized GCQDs (cell cytoplasm and nucleus) on MCF-7 breast cancer cell lines and high biocompatibility on L929 normal cells.

* Corresponding author.
E-mail addresses: os.kushwaha@ncl.res.in, omkar2ncl@gmail.com (O.S. Kushwaha).
[1] These authors have contributed equally to the work.

http://dx.doi.org/10.1016/j.apmt.2016.07.001
2352-9407/© 2016 Elsevier Ltd. All rights reserved.

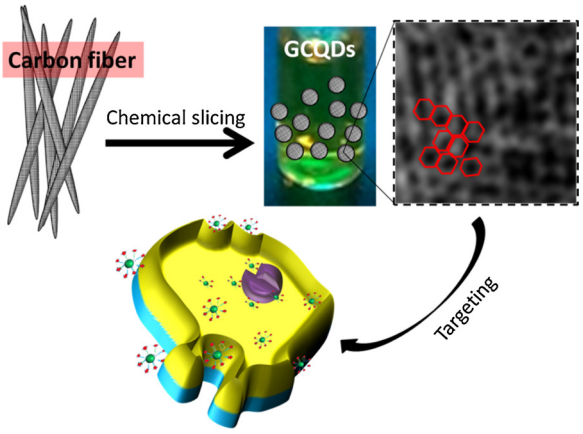

Scheme 1. Diagram depicting synthesis process of green fluorescent carbon quantum/nano dots (GCQDs) and targeting approach.

2. Materials and methods

2.1. Instrumentation and measurements

The synthesized GCQDs were systematically characterized with various physicochemical techniques. The size and morphology of nanostructures were examined by transmission electron microscopy operating at 200 kV. Samples for TEM were prepared by evaporating a droplet of sample onto 200 mesh carbon coated copper grid. Optical properties of GCQDs were characterized by UV/visible (Jasco V570) and photoluminescence (Scinco, Korea) spectrophotometry using standard quartz cuvette having a path length of 1 cm. Digital photographs were captured in UV cabinet. AFM images were obtained from atomic force microscope (PSIA XE-100) under tapping mode. The samples for AFM measurements were prepared by drop casting on clean silicon wafers surface after ultrasonic treatment (Equitron ultrasonic cleaner). Bio-imaging was performed with the help of fluorescence microscope (Axio Observer Z1, Carl Zeiss). Raman Spectrum was recorded from 800 to 3000 cm^{-1} on LabRAM Horiba JY HR-800 micro Raman spectrometer coupled with a microscope in reflectance mode with a 632.8 nm excitation He–Ne laser source. The dry sample was loaded on glass slide.

2.2. Synthesis and functionalization of green fluorescent CQDs (GCQDs)

In a 250 mL round bottom flask, 300 mg carbon fiber powder was mixed with 40 mL of concentrated H_2SO_4 and sonicated for 1 h at room temperature. The sonicated solution was injected slowly to 10 mL of HNO_3 followed by stirring for 12 h at room temperature. Freshly prepared 400 mL water was added (pH was adjusted to 7 with the help of Na_2CO_3 and NaOH) to the mixture. To remove the salts, the resulting solution was stirred in ice bath for 1 h followed by dialysis using dialysis bag (molecular weight cut-off 3000 Da) for 24 h. The final yield of GCQDs was found ~160 mg. The fluorescence effect was observed by passing 365 nm UV light in a UV cabinet. The surface functionalization of GCQDs with folic acid was carried out in stepwise manner. In order to activate carboxyl group, 0.2 M of 1-ethyl-3-(3-dimethylaminopropyl) carbodiimide and 0.4 M of N-hydroxysuccinimide were added in 100 mg of folic acid dissolved in 50 mL of MPW under constant stirring for 24 h at room temperature. Freshly prepared 10 mL solution of amine functionalized GCQDs (GCQDs-NH_2) was prepared by mixing of 1 M PEI with 10 mL of GCQDs and added dropwise to the above activated folic acid solution under constant stirring at room temperature for another 12 h. A solution of GCQDs-FA was obtained and freeze dried for further studies. The activation of folic acid and anchoring on GCQDs-NH_2 reactions were protected from direct light.

2.3. Cell culture

The normal L929 cells and MCF-7 cancer cells were cultured in regular Roswell Park Memorial Institute media (RPMI) 1640 medium supplemented with 10% Fetal Bovine serum and penicillin/streptomycin, under 5% CO_2 atmosphere at 37 °C.

2.4. In vitro *cytotoxicity assay*

In vitro cytotoxicity studies were performed over L929 cells using 24 h MTT assay. Cells were seeded at density of 2×10^4 cells per well of 96 well plate. 100 μL of different concentrations (10–1000 μg/mL) of GCQDs dispersed in media (incubated overnight, 5% CO_2 and 37 °C) were added into wells followed by 24 h incubation. After, incubated wells were washed off with PBS and 20 μL of MTT dye was added. Formazan crystals formed after 4 h were dissolved by 200 μL of DMSO. Optical absorbance was recorded at 570 nm and 690 nm using microplate reader (Tecan Infinite 200 PRO). Percentage cell viability was calculated in reference to untreated cells (negative control).

2.5. Cellular uptake of GCQDs

To ensure the cell targeting performance, folic acid was chosen as a targeting ligand and MCF-7 cells were treated with folic acid functionalized GCQDs (GCQDs-FA). Before this study the MCF-7 cells were seeded in 96 well plates at density of 2×10^4 cells/well and incubated overnight in incubator maintained at 5% CO_2 and 37 °C. Next day, wells were washed off with PBS and 100 μL of 20 μg/mL of GCQDs-FA was added. After 3 h and 12 h, wells were washed off with PBS twice to remove unbound particles. Thereafter, 4% paraformaldehyde solution was added to the cells and after 10 min of incubation nuclei were stained with 4, 6-diamidino-2-phenylindole (DAPI). Cover slip was then mounted over a drop of 70% glycerol on glass slide to fix the phase of the cell. Images were captured using fluorescence microscope (Axio Observer Z1, Carl Zeiss).

3. Results and discussion

3.1. Microscopic characterization of GCQDs

The morphology (size, shape and thickness) of GCQDs were confirmed by TEM and AFM (Fig. 1). TEM image revealed uniform distribution of GCQDs with an average particle size of ~3 nm (Fig. 1a) which was summarized in a histogram (Fig. 1b). The AFM image exhibits the topographical morphology of GCQDs (Fig. 1c). The heights between 0.5 nm and 2.5 nm as depicted from height distribution histogram correspond to 1–2 layers of GCQDs (Fig. 1d). The HRTEM images (Fig. 1e and f) and lattice parameter of 0.24 nm (Fig. 1g) demonstrated clear fringe gaps and honeycomb frameworks having hexagonal architectures which are attributed to crystalline structures [49–51].

3.2. Spectroscopic characterization of GCQDs

Further, UV–Vis spectrum of GCQDs (Fig. 2a) shows absorption peaks centered at λ_{max} 230 nm and λ_{max} 310 nm are attributed to the π–π^* transitions (of aromatic sp^2 domains) of the C=C band and n–π^* transitions of C=O band respectively [52,29] thus, indicate the presence of π-conjugated frameworks and carbonyl functional groups. Raman spectrum of GCQDs revealed the presence of sp^2 and

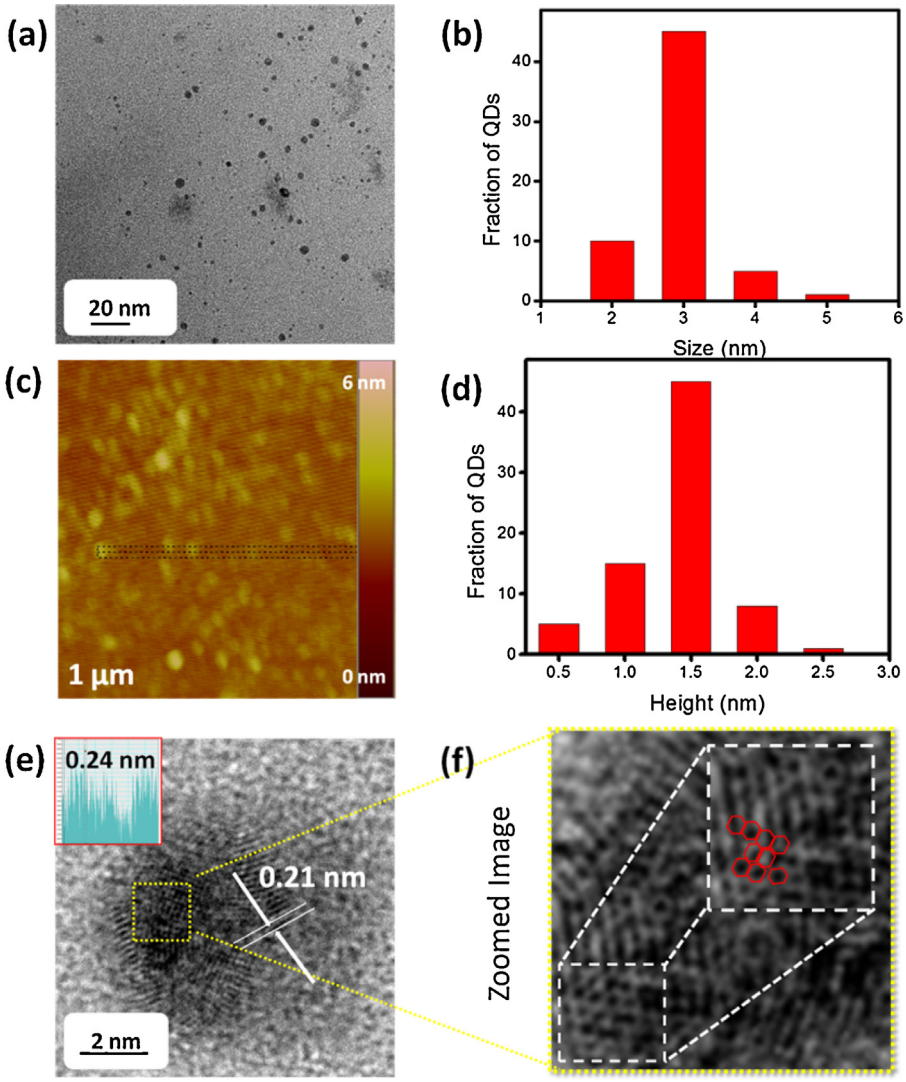

Fig. 1. Microscopic characterization of GCQDs (a) TEM image, (b) size distribution histogram (~3 nm), (c) AFM image (d) height distribution (thickness ~ 1.5 nm), (e, f) lattice fringe gap (~0.2 nm) and HRTEM image, and (g) zoomed HRTEM image with honey comb frameworks.

sp^3 carbon domains with D-band at 1324 cm^{-1} and a low intensity G-band at 1580 cm^{-1} (Fig. 2a, insert). The purity of GCQDs was confirmed from I_D/I_G value (0.84) and the absence of 2D peak.

Excitation with a wavelength of 430 nm showed a significant photoluminescence emission (green fluorescence) at 520 nm (Fig. 2b, black curve) being attributed to the fluorescence nature of GCQDs [6,52,29]. The presence of sp^2 and sp^3 carbon clusters in definite ratios in the GCQDs lead to its fluorescence [8,53]. Moreover, the photoluminescence spectra (Fig. 2b, red curve) of GCQDs taken after interval of 30 days showed similar photoluminescence intensity at 520 nm hence revealed good photostability and water dispersibility of GCQDs. Further, a prolonged photoluminescence stability of GCQDs was confirmed by the green fluorescence observed after a year (Fig. 2c, digital photographs). Under visible light, GCQDs showed brownish color whereas under UV light, (λ_{ex} 365 nm) GCQDs showed green fluorescence (Fig. 2c). The absence of aggregation and particle settling in aqueous solution of GCQDs was observed under visible light even after 30 days which revealed its high dispersibility behavior (Fig. 2b). Emission peak broadening observed under various pH conditions is attributed to the existence of multiple edges on GCQDs. In acidic pH (2–6) an increase in PL intensity whereas in basic pH (8–12) decrease in PL intensity was observed, attributed to proximate environment of GCQDs (presence of H^+/OH^- ions in solution) which may also influence the fluorescence quenching [54–57].

3.3. Photostability of aqueous suspension of GCQDs

The extra-high photostability of aqueous suspension of GCQDs (under visible light) at room temperature even after one year with a strong PL opens tremendous scope for future applications (Fig. 2b and c). Additionally, GCQDs showed sensitivity toward any change in pH of dispersion media. A slight red shift in emission wavelength and a significant blue shift in intensity due to change in pH (2–12) made it a potential candidate for early stage diagnosis of cancer. To the best of our knowledge, we firstly show high fluorescence activity of synthesized GCQDs at acidic pH (2–4) thus mimicking cancer cell environment (Fig. 2d). Moreover, change in color from light brown to dark brown with increase in pH (from 2 to 12, under visible light) may be attributed to the change in electronic transition of π–π^* and n–π^* in GCQDs. Once exposed to the excitation wavelengths in the range of 280–430 nm, GCQDs showed a drop in green fluorescence with an emission around 520 nm when pH of the GCQDs solution adjusted to alkaline from acidic (Fig. 3a–c). The exploitation of excitation wavelengths ensures the possibility of electronic transitions between HOMO and LUMO, and the

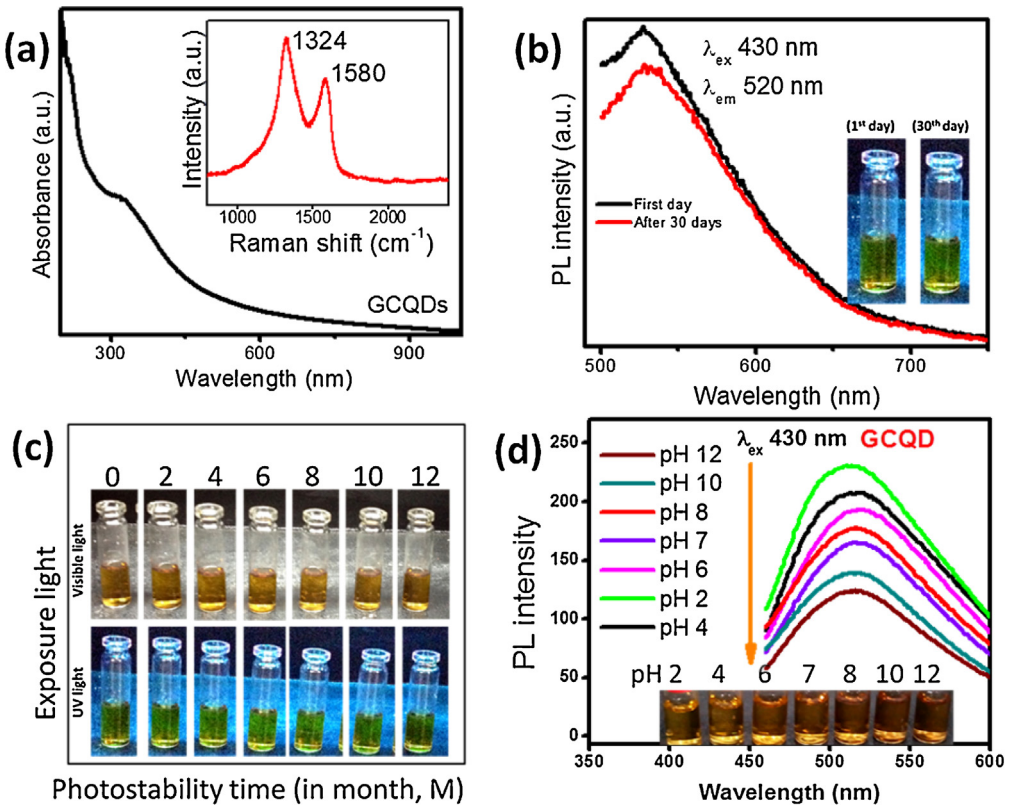

Fig. 2. Spectroscopic characterization of GCQDs (a) UV–Vis and Raman spectra (insert, Raman G and D bands), (b) green fluorescence, λ_{em} = 520 nm, (c) digital photographs showing photoluminescence stability up to 12 months, taken under UV and visible light, (d) pH (2–12) dependent fluorescence activity and digital photographs of water dispersed GCQDs.

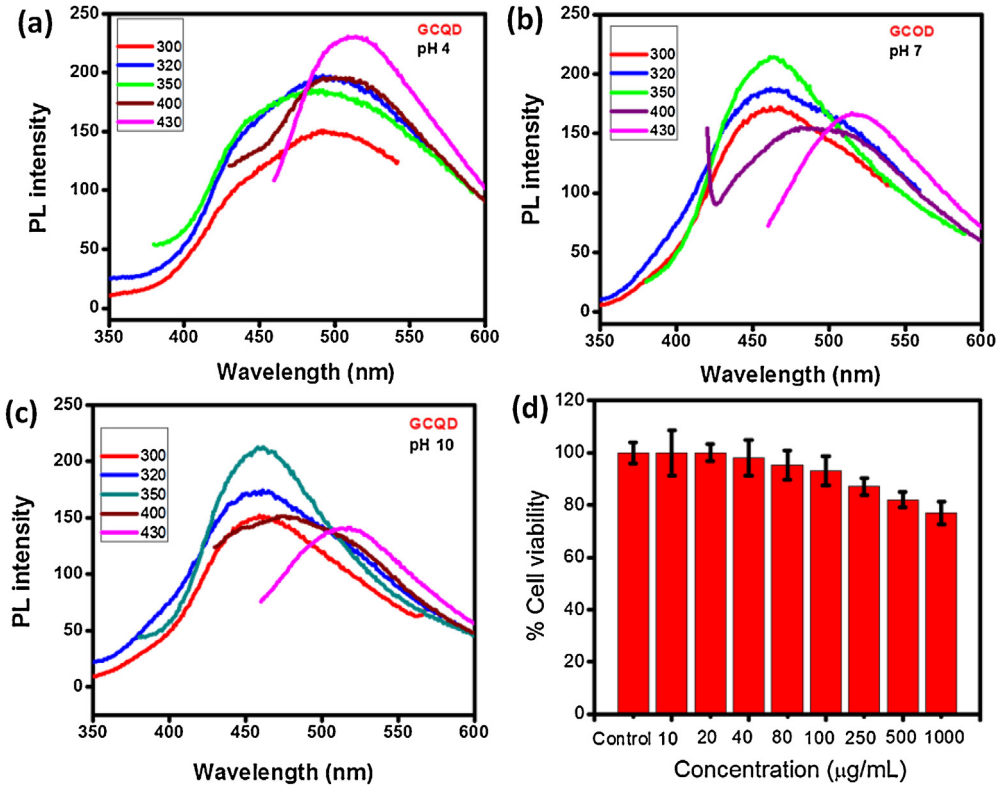

Fig. 3. (a, b and c) photoluminescence of GCQDs at pH 4, 7 and 10 respectively under different excitation wavelengths, emissions are observed in green fluorescence regions, (d) % cell viability assay of GCQDs on normal L929 cell lines.

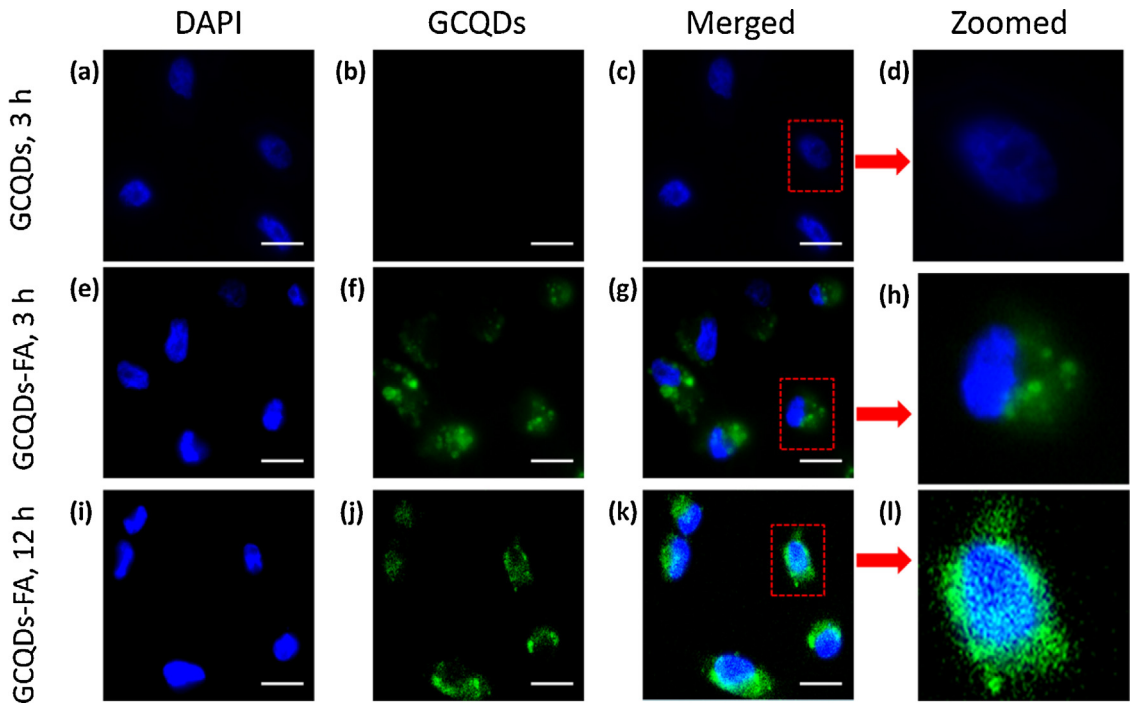

Fig. 4. Fluorescence microscopic images of MCF-7 cancer cells (a–d) GCQDs 3 h, (e–h) cells treated with GCQDs-FA for 3 h and (i–l) cells treated with GCQDs-FA for 12 h. Nucleus stained blue using DAPI and green fluorescence is due to GCQDs-FA. Scale bar is 10 μm.

peak shift in fluorescence may be corroborated to multiple electron transitions.

3.4. In vitro *cytotoxicity studies*

In order to access the viability of the GCQDs as potential bioimaging probe, *in vitro* cytotoxicity studies were carried out with fibroblastic normal L929 cell line by using MTT assay (for 24 h, 2×10^4 cells per well) at different concentrations (10–1000 μg/mL). The cell viability was calculated to be 100% in the control cells (in absence of GCQDs) and without any significant effects (Fig. 3d and Table S1). The average cell viability was found 80% after 24 h incubation at highest concentrations (1000 μg/mL) of GCQDs. The above results demonstrated high potential of GCQDs for optoelectronics and bio-medical applications.

3.5. In vitro *cell targeting and bio-imaging performance of GCQDs on MCF-7 breast cancer cells*

Further, evaluation of *in vitro* cell targeting and bio-imaging performance of GCQDs on MCF-7 breast cancer cells was carried out by using folic acid (FA) as a targeting ligand (Fig. 4). To understand the effect of FA on targeting ability, GCQDs and GCQDs-FA were incubated for 3 h (20 μg/mL) followed by fluorescence microscopy imaging. After 3 h of incubation, GCQDs showed lack of targeting ability which was evident by the absence of green fluorescence in the cell interior (Fig. 4a–d). Whereas, when GCQDs were functionalized with FA (a folate receptor ligand), an excellent targeting ability in cell cytoplasm was revealed by high green fluorescence after 3 h of incubation (Fig. 4e–h). Moreover, green fluorescence was observed in the cell cytoplasm and nucleus when incubation time was increased up to 12 h, confirming dual targeting ability of GCQDs which may be due to the high water solubility of the GCQDs-FA (Fig. 4i–l). Here, the enhanced visibility of green fluorescence in late endosome of MCF-7 cancer cell indicates the successful targeting ability of GCQDs-FA. Further, the appearance of green fluorescence in close proximity to the nucleus indicates the invasion ability of GCQDs-FA in the nucleus which makes it a potential candidate for targeted drug delivery for cancer theranostics. The presence of GCQDs-FA in cytoplasm and near to nucleus noticeably reflected their cell targeting capability (zoomed images, Fig. 4 and Table S2).

4. Conclusions

Green fluorescence of GCQDs-FA in MCF-7 breast cancer cells observed under fluorescence microscopy imaging is in accordance with the green fluorescence of acidic aqueous suspension of GCQDs obtained in PL spectra. We have demonstrated a one pot large scale synthesis for producing green fluorescent carbon quantum dots (GCQDs) of ~3 nm in size. The synthesis process ensured (1) one pot process (>50% conversion efficiency), (2) ambient reaction conditions, (3) excellent green photoluminescence and prolonged stability, (4) good water solubility and (5) superior biocompatibility. Due to low toxicity and good fluorescent nature, the GCQDs-FA was successfully used for targeted *in vitro* cell imaging (MCF-7 breast cancer cells). Further, excellent cancer cell cytoplasm and nucleus targeting performance of folic acid functionalized GCQDs (GCQDs-FA) has been demonstrated. A dual targeting ability (cytoplasm and nucleus) by using GCQDs-FA as a single platform has been observed.

Conflict of interest

The authors do not have any conflict of interest.

Acknowledgements

Authors acknowledge UGC, CSIR and DBT, India for partial financial support, and director CSIR-NCL for providing infrastructure.

Appendix A. Supplementary data

Supplementary data associated with this article can be found, in the online version, at doi:10.1016/j.apmt.2016.07.001.

References

[1] P. Rai, S. Mallidi, X. Zheng, R. Rahmanzadeh, Y. Mir, S. Elrington, A. Khurshid, T. Hasan, Development and applications of photo-triggered theranostic agents, Adv. Drug Del. Rev. 62 (2010) 1094.
[2] E.J. Hall, D.J. Brenner, Cancer risks from diagnostic radiology, Br. J. Radiol. 81 (2008) 362.
[3] G.Z. Ge, H.J. Xia, B.L. He, H.L. Zhang, W.J. Liu, M. Shao, C.Y. Wang, J. Xiao, F. Ge, F.B. Li, Y. Li, Generation and characterization of a breast carcinoma model by PyMT overexpression in mammary epithelial cells of tree shrew, an animal close to primates in evolution, Int. J. Cancer 138 (2016) 642.
[4] D. Yan, B. Lei, B. Chen, X.-J. Wu, Z. Liu, N. Li, J. Ge, Y. Xue, Y. Du, Z. Zheng, H. Zhang, Synthesis of high-quality lanthanide oxybromides nanocrystals with single-source precursor for promising applications in cancer cells imaging, Appl. Mater. Today 1 (2015) 20.
[5] J.G. Hardy, E. Larraneta, R.F. Donnelly, N. McGoldrick, K. Migalska, M.T. McCrudden, L. Donnelly, C.P. McCoy, Hydrogel-forming microneedle arrays made from light-responsive materials for on-demand transdermal drug delivery, Mol. Pharm. 13 (2016) 907.
[6] R. Liu, D. Wu, X. Feng, K. Müllen, Bottom-up fabrication of photoluminescent graphene quantum dots with uniform morphology, J. Am. Chem. Soc. 133 (2011) 15221.
[7] J. Liu, L. Cao, G.E. LeCroy, P. Wang, M.J. Meziani, Y. Dong, Y. Liu, P.G. Luo, Y.P. Sun, *ACS* Carbon "quantum" dots for fluorescence labeling of cells, Appl. Mater. Interfaces 7 (2015) 19439.
[8] J. Peng, W. Gao, B.K. Gupta, Z. Liu, R.R. Aburto, L. Ge, L. Song, L.B. Alemany, X. Zhan, G. Gao, S.A. Vithayathil, B.A. Kaipparettu, A.A. Marti, T. Hayashi, J.J. Zhu, P.M. Ajayan, Graphene quantum dots derived from carbon fibers, Nano Lett. 12 (2012) 844.
[9] J.L. Vivero-Escoto, W.J. Rieter, H. Lau, R.H. Phillips, W. Lin, Biodegradable polysilsesquioxane nanoparticles as efficient contrast agents for magnetic resonance imaging, Small 9 (2013) 3523.
[10] I.L. Medintz, H.T. Uyeda, E.R. Goldman, H. Mattoussi, Quantum dot bioconjugates for imaging, labelling and sensing, Nat. Mater. 4 (2005) 435.
[11] U. Resch-Genger, M. Grabolle, S. Cavaliere-Jaricot, R. Nitschke, T. Nann, Quantum dots versus organic dyes as fluorescent labels, Nat. Methods 5 (2008) 763.
[12] O.S. Kushwaha, C.V. Avadhani, R.P. Singh, Preparation and characterization of self-photostabilizing UV-durable bionanocomposite membranes for outdoor applications, Carbohyd. Polym. 123 (2015) 164.
[13] S. Bouccara, G. Sitbon, A. Fragola, V. Loriette, N. Lequeux, T. Pons, Enhancing fluorescence in vivo imaging using inorganic nanoprobes, Curr. Opin. Biotechnol. 34 (2015) 65.
[14] S.P. Lonkar, O.S. Kushwaha, A. Leuteritz, G. Heinrich, R.P. Singh, Self photostabilizing UV-durable MWCNT/polymer nanocomposites, RSC Adv. 2 (2012) 12255.
[15] A.T. Lam, J. Yoon, E.O. Ganbold, D.K. Singh, D. Kim, K.H. Cho, S.Y. Lee, J. Choo, K. Lee, S.W. Joo, Colloidal gold nanoparticle conjugates of gefitinib, Colloid Surf. B 123 (2014) 61.
[16] J. Zhang, C. Li, X. Zhang, S. Huo, S. Jin, F.F. An, X. Wang, X. Xue, C.I. Okeke, G. Duan, F. Guo, In vivo tumor-targeted dual-modal fluorescence/CT imaging using a nanoprobe Co-loaded with an aggregation-induced emission dye and gold nanoparticles, Biomaterials 42 (2015) 103.
[17] Z. Wan, S. Lu, D. Zhao, Y. Ding, P. Chen, Arginine-rich ionic complementary peptides as potential drug carriers: impact of peptide sequence on size, shape and cell specificity, Nanomed. Nanotech. Biol. Med. 12 (2016) 1479.
[18] C. He, K. Lu, W. Lin, Nanoscale metal–organic frameworks for real-time intracellular pH sensing in live cells, J. Am. Chem. Soc. 136 (2014) 12253.
[19] J. Nam, N. Won, J. Bang, H. Jin, J. Park, S. Jung, S. Jung, Y. Park, S. Kim, Surface engineering of inorganic nanoparticles for imaging and therapy, Adv. Drug Del. Rev. 65 (2013) 622.
[20] P. Wu, T. Zhao, S. Wang, X. Hou, Semicondutor quantum dots-based metal ion probes, Nanoscale 6 (2014) 43.
[21] A.H. Loo, Z. Sofer, D. Bouša, P. Ulbrich, A. Bonanni, M. Pumera, Carboxylic carbon quantum dots as a fluorescent sensing platform for DNA detection, ACS Appl. Mater. Interfaces 8 (2016) 1951.
[22] J. Weingart, P. Vabbilisetty, X.L. Sun, Membrane mimetic surface functionalization of nanoparticles: methods and applications, Adv. Colloid Interface Sci. 197 (2013) 68.
[23] T.R. Kuo, S.Y. Sung, C.W. Hsu, C.J. Chang, T.C. Chiu, C.C. Hu, One-pot green hydrothermal synthesis of fluorescent nitrogen-doped carbon nanodots for in vivo bioimaging, Anal. Bioanal. Chem. 408 (2016) 77.
[24] A. Cayuela, M.L. Soriano, C. Carrillo-Carrión, M. Valcárcel, Semiconductor and carbon-based fluorescent nanodots: the need for consistency, Chem. Commun. 52 (2016) 1311.
[25] Y. Guo, Z. Wang, H. Shao, X. Jiang, Hydrothermal synthesis of highly fluorescent carbon nanoparticles from sodium citrate and their use for the detection of mercury ions, Carbon 52 (2013) 583.
[26] P. Innocenzi, L. Malfatti, D. Carboni, Graphene and carbon nanodots in mesoporous materials: an interactive platform for functional applications, Nanoscale 7 (2015) 12759.
[27] S. Zhu, X. Zhao, Y. Song, S. Lu, B. Yang, Beyond bottom-up carbon nanodots: citric-acid derived organic molecules, Nano Today 11 (2016) 128.
[28] Y. Zhong, F. Peng, F. Bao, S. Wang, X. Ji, L. Yang, Y. Su, S.T. Lee, Y. He, Large-scale aqueous synthesis of fluorescent and biocompatible silicon nanoparticles and their use as highly photostable biological probes, J. Am. Chem. Soc. 135 (2013) 8350.
[29] H. Li, X. He, Z. Kang, H. Huang, Y. Liu, J. Liu, S. Lian, C.H.A. Tsang, X. Yang, S.T. Lee, Water-soluble fluorescent carbon quantum dots and photocatalyst design, Angew. Chem. Int. Ed. 49 (2010) 4430.
[30] S.T. Yang, L. Cao, P.G. Luo, F.S. Lu, X. Wang, H.F. Wang, M.J. Meziani, Y.F. Liu, G. Qi, Y.P. Sun, Carbon dots for optical imaging in vivo, J. Am. Chem. Soc. 131 (2009) 11308.
[31] L. Tian, D. Ghosh, W. Chen, S. Pradhan, X.J. Chang, S.W. Chen, Nanosized carbon particles from natural gas soot, Chem. Mater. 21 (2009) 2803.
[32] L. Tian, Y. Song, X.J. Chang, S.W. Chen, Hydrothermally enhanced photoluminescence of carbon nanoparticles, Scr. Mater. 62 (2010) 883.
[33] M. Bottini, C. Balasubramanian, M.I. Dawson, A. Bergamaschi, S. Bellucci, T. Mustelin, Isolation and characterization of fluorescent nanoparticles from pristine and oxidized electric arc-produced single-walled carbon nanotubes, J. Phys. Chem. B 110 (2006) 831.
[34] A.M. Derfus, W.C.W. Chan, S.N. Bhatia, Probing the cytotoxicity of semiconductor quantum dots, Nano Lett. 4 (2004) 11.
[35] A. Mewada, S. Pandey, S. Shinde, N. Mishra, G. Oza, M. Thakur, M. Sharon, M. Sharon, Green synthesis of biocompatible carbon dots using aqueous extract of *Trapa bispinosa* peel, Mater. Sci. Eng. C 33 (2013) 2914.
[36] M. Zhang, L. Bai, W. Shang, W. Xie, H. Ma, Y. Fu, D. Fang, H. Sun, L. Fan, M. Han, C. Liu, Facile synthesis of water-soluble, highly fluorescent graphene quantum dots as a robust biological label for stem cells, J. Mater. Chem. 22 (2012) 7461.
[37] K.M. Tripathi, N.R. Gupta, S.K. Sonkar, Smart Materials for Waste Water Applications, John Wiley & Sons, 2016, pp. 127–153.
[38] S. Qu, X. Wang, Q. Lu, X. Liu, L. Wang, A biocompatible fluorescent ink based on water-soluble luminescent carbon nanodots, Angew. Chem. Int. Ed. 124 (2012) 12381.
[39] Q. Zhang, X. Wang, P.Z. Li, K.T. Nguyen, X.J. Wang, Z. Luo, H. Zhang, N.S. Tan, Y. Zhao, Biocompatible, uniform, and redispersible mesoporous silica nanoparticles for cancer-targeted drug delivery in vivo, Adv. Funct. Mater. 24 (2014) 2450.
[40] Z. Cheng, A. Zaki Al, J.Z. Hui, V.R. Muzykantov, A. Tsourkas, Multifunctional nanoparticles: cost versus benefit of adding targeting and imaging capabilities, Science 338 (2012) 903.
[41] F. Wang, G.M. Pauletti, J. Wang, J. Zhang, R.C. Ewing, Y. Wang, D. Shi, Dual surface-functionalized janus nanocomposites of polystyrene/Fe_3O_4@ SiO_2 for simultaneous tumor cell targeting and stimulus-induced drug release, Adv. Mater. 25 (2013) 3485.
[42] J.H. Lee, A. Sahu, C. Jang, G. Tae, The effect of ligand density on in vivo tumor targeting of nanographene oxide, J. Control Rel. 209 (2015) 219.
[43] Z. Wang, B. Xu, L. Zhang, J. Zhang, T. Ma, J. Zhang, X. Fu, W. Tian, Folic acid-functionalized mesoporous silica nanospheres hybridized with AIE luminogens for targeted cancer cell imaging, Nanoscale 5 (2013) 2065.
[44] S. Yao, Y. Hu, G. Li, Flowing electrolytic synthesis of fluorescent carbon nanoparticles and carbon nanosheets, Electrochim. Acta 155 (2015) 305.
[45] H. Xu, Q. Li, L. Wang, Y. He, J. Shi, B. Tang, C. Fan, Nanoscale optical probes for cellular imaging, Chem. Soc. Rev. 43 (2014) 2650.
[46] X. Li, M. Rui, J. Song, Z. Shen, H. Zeng, Carbon and graphene quantum dots for optoelectronic and energy devices: a review, Adv. Funct. Mater. 25 (2015) 4929.
[47] S. Zhu, J. Shao, Y. Song, X. Zhao, J. Du, L. Wang, H. Wang, K. Zhang, J. Zhang, B. Yang, Investigating the surface state of graphene quantum dots, Nanoscale 7 (2015) 7927.
[48] S. Wuttke, S. Braig, T. Preiß, A. Zimpel, J. Sicklinger, C. Bellomo, J.O. Rädler, A.M. Vollmar, T. Bein, MOF nanoparticles coated by lipid bilayers and their uptake by cancer cells, Chem. Commun. 51 (2015) 15752.
[49] L. Zhang, Y. Xing, N. He, Y. Zhang, Z. Lu, J. Zhang, Z. Zhang, Preparation of graphene quantum dots for bioimaging application, J. Nanosci. Nanotechnol. 12 (2012) 2924.
[50] M. Bacon, S.J. Bradley, T. Nann, Graphene quantum dots, Part. Part. Syst. Charact. 31 (2014) 415.
[51] X. Tan, Y. Li, X. Li, S. Zhou, L. Fan, S. Yang, Electrochemical synthesis of small-sized red fluorescent graphene quantum dots as a bioimaging platform, Chem. Commun. 51 (2015) 2544.
[52] Q. Liang, W. Ma, Y. Shi, Z. Li, X. Yang, Easy synthesis of highly fluorescent carbon quantum dots from gelatin and their luminescent properties and applications, Carbon 60 (2013) 421.
[53] Z.L. Wu, M.X. Gao, T.T. Wang, X.Y. Wan, L.L. Zheng, C.Z. Huang, A general quantitative pH sensor developed with dicyandiamide N-doped high quantum yield graphene quantum dots, Nanoscale 6 (2014) 3868.

[54] Z. Yan, J. Shu, Y. Yu, Z. Zhang, Z. Liu, J. Chen, Preparation of carbon quantum dots based on starch and their spectral properties, Luminescence 30 (2015) 388.
[55] Z. Lei, S. Xu, J. Wan, P. Wu, Facile synthesis of N-rich carbon quantum dots by spontaneous polymerization and incision of solvents as efficient bioimaging probes and advanced electrocatalysts for oxygen reduction reaction, Nanoscale 8 (2016) 2219.
[56] C. Wang, Z. Xu, H. Cheng, H. Lin, M.G. Humphrey, C. Zhang, A hydrothermal route to water-stable luminescent carbon dots as nanosensors for pH and temperature, Carbon 82 (2015) 87.
[57] Z. Song, F. Quan, Y. Xu, M. Liu, L. Cui, J. Liu, N. Multifunctional, S Co-doped carbon quantum dots with pH- and thermo-dependent switchable fluorescent properties and highly selective detection of glutathione, Carbon 104 (2016) 169.